

# Programmable 3D Stochastic Fluidic Assembly of cm-scale Modules

Michael T. Tolley, Hod Lipson, *Member, IEEE*

**Abstract**—Self-reconfiguring modular robotic systems offer a potential route to achieving *programmable matter*, i.e. a substance the shape and properties of which can be tuned as required to achieve a particular task. However, most modular robotic system designs rely on deterministic module motions which place significant power, control, and actuation requirements on the individual modules. This leads to relatively large modules and low target structure resolution. Here we experimentally demonstrate an alternative approach based on stochastic assembly in which modules assemble into target structures in a fluidic tank. This system employs ambient fluid motion for module transportation. Assembly is directed by controlling the fluid flow through an active assembly substrate with an array of valves. Different valving programs are used with feedback from pressure sensors to achieve the automated hierarchical assembly of non-planar 3D structures.

## I. INTRODUCTION

RECENTLY, there has been a great deal of interest in the concept of *programmable matter*, with a number of research groups pursuing a variety of approaches to achieving a robotic system with programmable morphology [1]-[14]. One potential route to achieving programmable matter is to employ stochastic assembly [14]-[7]. Inspired by nature, stochastic approaches achieve the assembly of robotic modules by taking advantage of stochastic environmental motions for component transportation. This reduces the power, actuation, and computation requirements on the modules, allowing them to be produced more cheaply, and at smaller scales, thereby increasing the resolution of the assembled structures.

Stochastic Fluidic Assembly (SFA) represents a promising approach to achieving target geometries for programmable matter [8]-[13]. Previous SFA work has achieved the assembly of a small number of 10 to 20 cm scale modules [8],[9], and planar assembly of 500 micron scale modules [10],[11]. Computational studies have also explored control approaches for the assembly of SFA modules capable of manipulating internal fluid flow [12],[13].

In this paper, we present results demonstrating the SFA of simple, completely passive, cm scale modules. The experimental system, and initial assembly results, were

presented in [14]. Here we extend these results with three sets of experiments. First, in Section II we review the design of the experimental system and control software and describe upgrades that enable new capabilities. Section III provides an overview of the control approach for the experiments. Section IV then presents the first set of experiments performed with this system to demonstrate the robust assembly of nonplanar 3D structures with minimal human intervention. In Section V we describe the second set of experiments demonstrating the parallel hierarchical assembly of 3D structures. Section VI describes a third set of experiments which use sensor feedback to achieve the fully automated assembly of 3D structures. Three different assembly programs are tested and the corresponding experimental results are discussed. Section VII comprises an overall discussion and conclusion of these results.

## II. SYSTEM DESIGN

The design of our SFA system is discussed in detail in [14]. However, significant modifications were made to this experimental apparatus to enable the experiments described in this paper. In this section, we summarize the overall design of the SFA system, focussing on the new aspects.

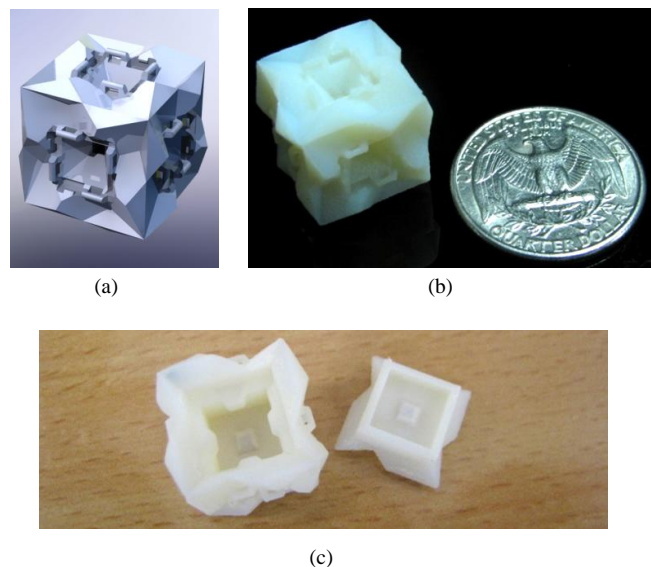


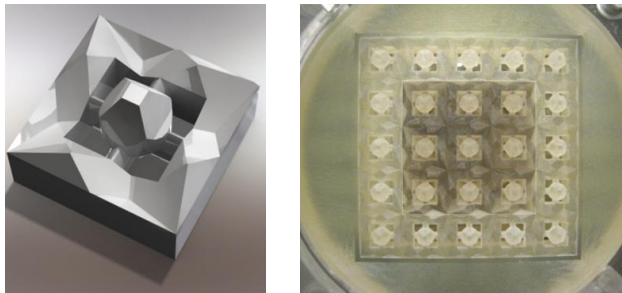
Fig. 1. SFA Modules. (a) Computer aided design and (b) 3D printed version of assembly module with a length of 15 mm. Alignment patterns and latches on each face allow cubes to self-align and bond together under the influence of fluidic assembly forces. (c) A two-piece design traps an internal air pocket to achieve neutral-buoyancy.

This work was funded by the DARPA grant number W911NF-08-1-0140 (Programmable Matter Program). M. T. Tolley would also like to thank the Canadian NSERC for their support through the PGS Program.

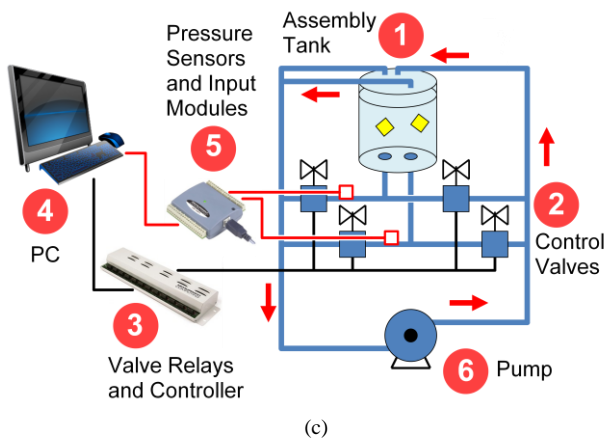
M. T. Tolley is with the Harvard University Microrobotics Laboratory, Cambridge, MA, 02138 USA (e-mail: mike.tolley@wyss.harvard.edu). H. Lipson is with the Computational Synthesis Laboratory, Cornell University, Ithaca, NY, 14853 USA (e-mail: hod.lipson@cornell.edu).

### A. Module Design

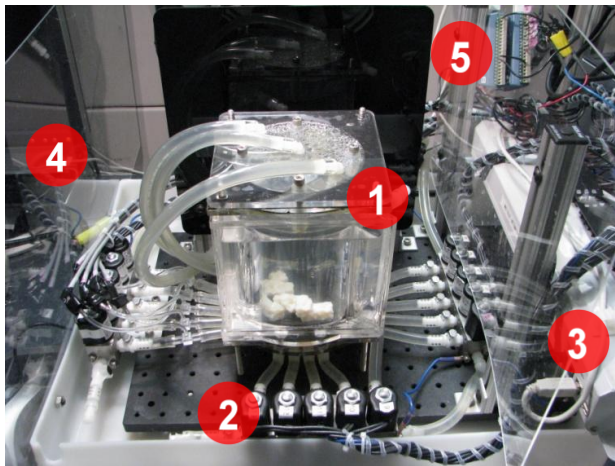
The assembly modules are cubes with an alignment patterns and passive compliant latches on each face [Fig. 1(a)]. Four-fold rotational symmetry in the face design allows any pair of faces from two cubes to mate in any orientation. These modules were printed on an Objet Connex 3D printer out of their Vera White acrylic-based photopolymer material. The modules have a side length of 15 mm [Fig. 1(b)]. A two-piece design is used to trap air in an internal pocket to achieve near-neutral buoyancy [Fig. 1(c)]. This facilitates the manipulation of larger assemblies with fluidic forces.



(a) (b)



(c)



(d)

Fig. 2. Experimental system. (a) CAD drawing of outlet port design. (b) Photograph of assembly substrate with nine active ports surrounded by 16 passive ports. (c) Schematic, and (d) photograph of experimental system with primary components identified.

### A. Stochastic Fluidic Assembly System

The SFA modules are assembled on an active assembly substrate consisting of an array of fluidic ports with alignment patterns that match those of the cubes [Fig. 2(a)]. The substrate consists of a three-by-three array of active ports surrounded by 16 passive ports [Fig. 2(b)]. A schematic of the system that controls the active ports so that they act as either sources or sinks is seen in Fig. 2(c). A pump provides high pressure flow to a set of control valves that can be opened to make the active ports serve as fluid sources. A second, complimentary set of solenoid valves can be opened to connect the ports to the low pressure end of the fluidic circuit, causing them to serve as sinks. An alternate path allows fluid to flow through the top of the tank when all of the valves are closed. The solenoids are controlled with a USB relay controller. Additionally, a set of pressure sensors provide feedback on the state of the active assembly ports (part no. PX40-50BHG5V, Omega Engineering, www.omega.com). This information is relayed to the control software with an A/D input modules (part no. USB-1208FS, Measurement computing, www.mccdaq.com). Part numbers and suppliers for all the components not specified above can be found in [14]. Fig. 2(d) is a photograph of the experimental system.

### B. Control Software

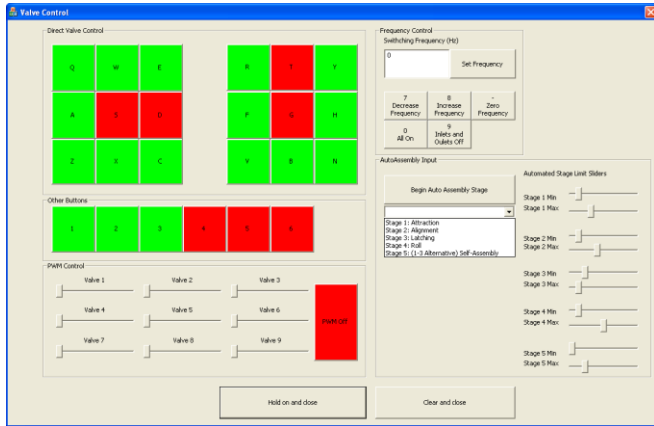
Custom control software was written in C++ to allow both manual and automated control of the SFA system. Fig. 3(a) is a screenshot of the graphical user interface (GUI). Two sets of nine buttons in the upper-left allow manual control of the inlet and outlet valves for the nine substrate ports.

One of the initial problems with the SFA approach is that friction/stiction would prevent the modules from aligning and latching when brought together. This problem was solved by rapidly opening and closing the inlet/outlet valves to pulsate the flow, short-timescale random motions to the random circulation flow in the assembly tank. The controls in the top-right of the GUI allow for control of the frequency of this pulsation.

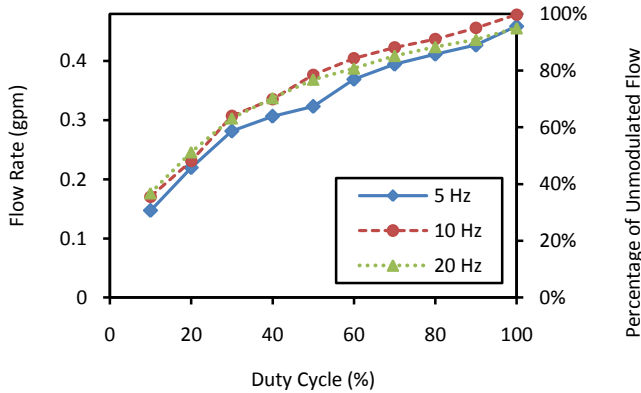
Another problem preventing successful assembly was that the resolution of the valve control was found to be too crude. Turning a source on adjacent to a sink would completely reject an attracted module. In order to achieve a more continuous range of control options, we implemented pulse-width modulation (PWM) of the control signals to the valves. We tested the PWM valve control by connecting a flow meter to the outlet of a valve and measuring the resulting flow rates for various duty cycle settings. Fig. 3(b) shows the results of these tests for PWM at three different frequencies (5 Hz, 10 Hz and 20 Hz). The data for all three cases follow approximately an exponential curve with a power of 0.5. Ideally, this relationship would be used to achieve a linear range of flow rates. However, actuation of the valves at frequencies higher than approximately 20 Hz was not possible. Nonetheless, the flow rates were monotonically increasing and fairly close to linear in the

duty cycle. This range of achievable flow rates was a great improvement over the previous on-off control. The sliders in the lower-left portion of the GUI allow manual adjustment of the strength of the source or sink flow at the nine substrate ports.

Finally, the controls on the lower-right of the GUI are for a set of open-loop subroutines used to achieve automated assembly, and for initiating of the automated assembly experiments. The high level control approach is discussed in detail in the next section.



(a)



(b)

Fig. 3. Control Software. (a) GUI used for both manual control of SFA system and for adjusting parameters of automated control algorithms. (b) Flow rates measured for PWM at various frequencies confirm this as a valid approach to achieving flow control between completely *off* and completely *on*.

### III. CONTROL ALGORITHMS

Our approach to achieving completely automated SFA was to minimize the feedback required for assembly. This was achieved by devising a set of open-loop algorithms to accomplish the various assembly tasks. This approach can be seen as a finite state machine (FSM) where feedback is only required to initiate the state transitions [Fig. 4(a)]. Each state represents a set of repeating valve sequences designed to achieve a particular assembly task, i.e. attraction, alignment,

latching, or release. Some of the inputs to the states (e.g. where to attract cubes) are determined by the overall assembly program.

For example, a particular program may initiate assembly by identifying the attraction locations at which point control transitions to the *Attract* state. The identified locations then become sinks while the rest of the substrate ports become sources. In order to agitate the cubes, the sources cycle between levels of low and high flow. Once cubes have been attracted to the desired locations (this can be identified either with human or sensor feedback), the software moves to the next stage of assembly (*Align*). Table I summarizes the four assembly states, required inputs, and the associated open-loop control algorithms. A fifth state *Align/Latch* is also listed that was developed to replace the separate *Align* and *Latch* states for the automated assembly experiments (see Section VI for details).

TABLE I  
FINITE-STATE-MACHINE OPEN-LOOP ASSEMBLY CONTROL ALGORITHMS

State	Inputs	Algorithm
Attract	Desired cube locations	<ul style="list-style-type: none"> <li>Open desired cube locations to low pressure</li> <li>Open all other ports to high pressure</li> <li>Modulate duty cycle of high pressure Loop through sources one at a time, increasing their strengths to <math>A_{max}</math>, then back down to <math>A_{min}</math> (for agitation)</li> <li>When one or more cubes have been attracted to desired locations, move to Align</li> </ul>
Align	Locations of mated and unmated cubes	<ul style="list-style-type: none"> <li>Open sinks at cube locations</li> <li>Also open source at mated cube location and increase its strength slowly until cubes align</li> <li>Done when cubes are aligned (go to latch), or a target location is no longer occupied by a cube (go to attract)</li> </ul>
Latch	Cube locations	<ul style="list-style-type: none"> <li>Open sinks at cube locations</li> <li>Open sources at cube locations</li> <li>Increase source strengths slowly to vibrate cubes until cubes latch (go to attract or release as dictated by assembly plan), or become misaligned (go to align)</li> </ul>
Release	Cube locations	<ul style="list-style-type: none"> <li>Open sources at cube locations</li> <li>Slowly increase sources to release structure from substrate</li> <li>For reorientation, attract to new location (attract), otherwise assembly is done</li> </ul>
Align/Latch	Location (s) of mated cube(s)	<ul style="list-style-type: none"> <li>Open sinks at desired cube locations</li> <li>Agitate flow with remaining ports, as in Attract</li> <li>Loop through sinks with attracted cubes, using PWM to switch them between sink and source to agitate the attracted cube and allow new cubes to align in adjacent locations</li> <li>Continue to shake attracted cubes until latched</li> <li>Done when all cubes are aligned (go to latch), or a target location is no longer occupied by a cube (go to attract)</li> </ul>

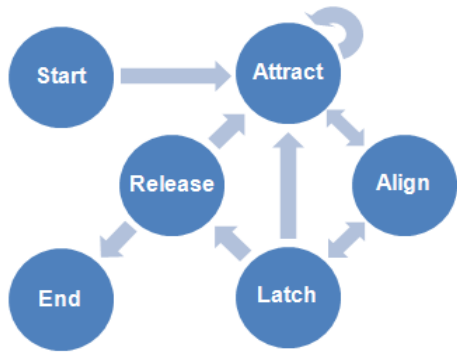


Fig. 4. Schematic of FSM approach to assembly control. Assembly consists of a sequence of four fundamental assembly operations corresponding to the four main states seen here. Each of the states runs open-loop valving sequences. Transitions between states are initiated in response to feedback on the state of the system according to the specific assembly program.

#### IV. ROBUST 3-D ASSEMBLY

One of the key aspects of our SFA system is that the same forces used to manipulate modules can also be used to manipulate assemblies. Because of this feature, a non-planar 3D structure can be assembled by releasing a 2D structure assembled on the substrate and re-orienting it into an upright position. New modules can then be added at the substrate to form 3D structure. To demonstrate this capability, we performed a set of experiments to assemble an L-shape, then reorient it upright on the substrate to add a fourth module [Fig. 5(a)]. In order to evaluate the robustness of this approach, we repeated this process 10 times consecutively and recorded the assembly times for each stage of assembly [Fig. 5(b)].

Fig. 5(a) shows a sequence of images that illustrate the 8 stages required for the assembly of the four-module target structure. (Note that some of these stages comprise multiple of the FSM states discussed in the previous section). This sequence of stages represents the overall program for the assembly of the structure shown in the last image. For these experiments, the transitions between the FSM states required to follow this program were initiated by a human observer.

Fig. 5(a) summarizes the time taken in each experiment to achieve the eight assembly stages depicted in Fig. 5(a). Each dataset represents one experiment, with the vertical axis representing the ordered assembly stages and the horizontal axis denoting the corresponding experimental time. Some of the experiments did not achieve all of the assembly stages. This is because an experiment was ended if an assembly came apart such that the entire sequence would have to be restarted from the beginning.

Overall, the target structure was completed in 60% of the experiments. The mean time to the final assembly stage was 442 s whereas the median was 339 s. (This is because the mean is largely affected by one outlier experiment that took much longer than the others.) Looking at the individual experiment times, we see that most experiments spent a similar amount of time on each stage. However, two

experiments took a relatively long time to get a second module aligned and one also took a long time to achieve successful reorientation. Comparing these results with the experiments described in [14], we see the upgraded experimental system and improved control strategies reduced the average pair assembly time from 346s to 165 s, and the three-module assembly time from 398 s to 281 s.

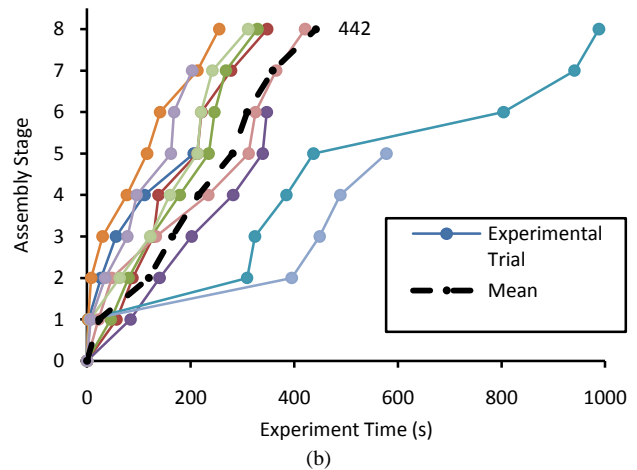
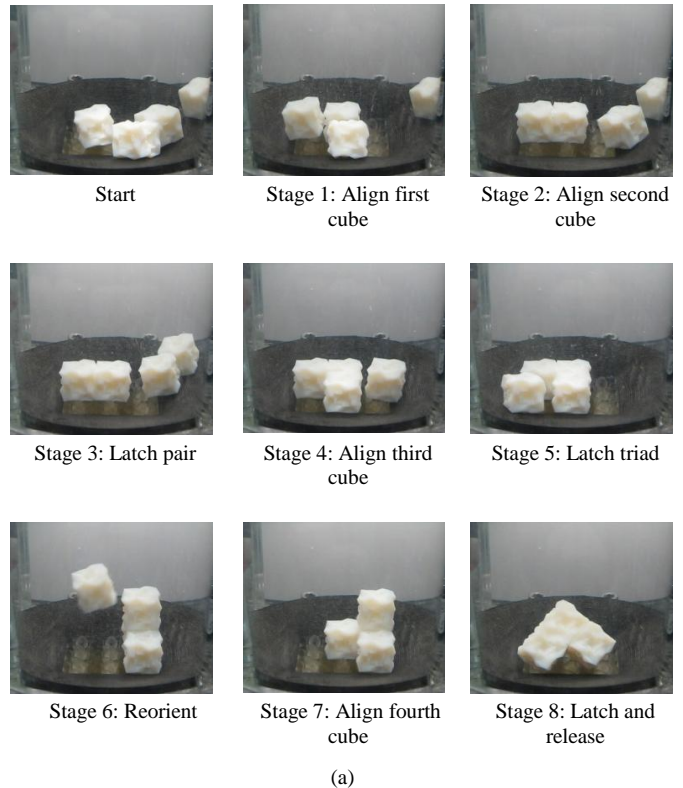
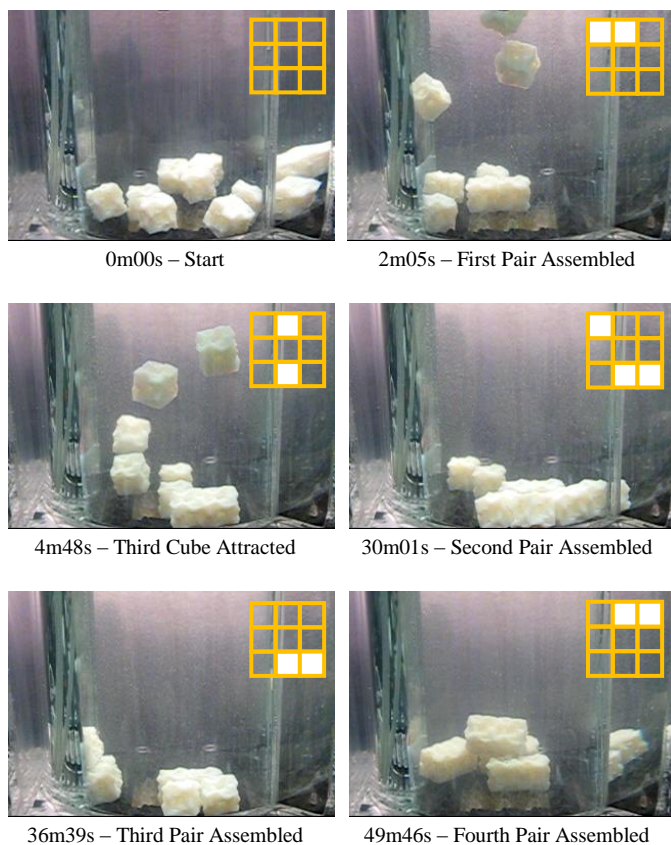


Fig. 5. Robust 3-D Assembly. (a) Sequence of images from a 3-D assembly experiment displaying the eight required assembly operations. (b) Plot of assembly times of 10 consecutive 3-D assembly experiments. Each data series represents one experiment. Data points indicate the time elapsed since the start of the experiment when the corresponding assembly stages were achieved. The mean dataset corresponds to the mean time taken to achieve each assembly stage.

### Hierarchical Stage 1



### Hierarchical Stage 2

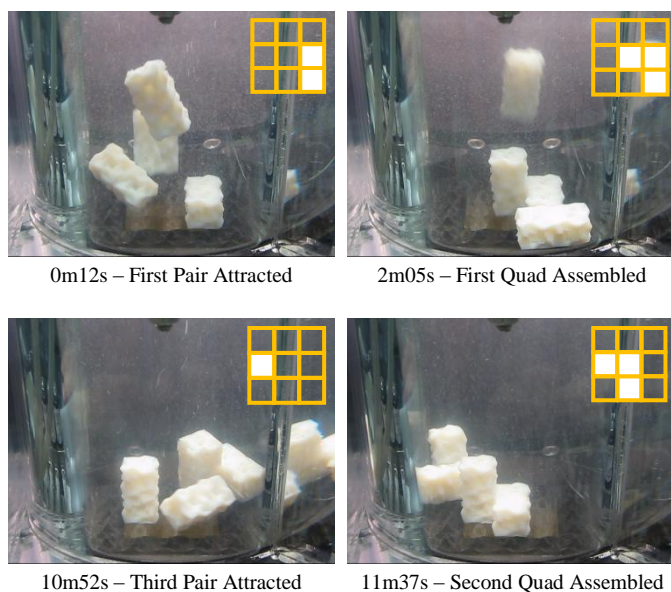


Fig. 6. Parallel Hierarchical 3D Assembly. Representative frames from two assembly experiments corresponding to the first stage and second stages of the parallel hierarchical assembly of two 3D structures. In the first stage, SFA is used to assemble eight individual modules into four pairs of modules simultaneously on the top and bottom rows of the array. In the second stage, these pairs are assembled into 3D structures. The grid on the upper-right hand corner of each image indicates the locations on the  $3 \times 3$  array of substrate ports that are occupied by modules.

## V. PARALLEL HIERARCHICAL 3D ASSEMBLY

One of the challenges of SFA highlighted by the results of the previous section is the slow assembly rates. Thus, serial assembly takes a long time when compared to deterministic assembly approaches. However, it may be possible to mitigate this disadvantage by employing parallel hierarchical assembly. Such an approach would assemble multiple sub-components in parallel to later be assembled into a final structure, significantly reducing the overall assembly time.

In order to demonstrate our system’s ability to achieve parallel hierarchical assembly, we conducted experiments to assemble structures that form the building blocks for subsequent assembly. In these experiments, the goal was to demonstrate the assembly of sub-structures comprising two modules, then to form two identical non-planar four-module structures from these sub-assemblies. These experiments were conducted using a similar approach to that described in the previous section, with a FSM control algorithm supervised by a human operator using visual feedback.

Fig. 6 presents frames from videos of the two stages of the parallel hierarchical stochastic fluidic assembly of two 3-D structures. The approach was to first assemble individual modules into pairs, then, as the second stage of hierarchical assembly, to assemble these pairs into four-module structures. Non-planar structures were achieved by attracting the pre-assembled pairs to the substrate in both horizontal and vertical positions, and latching them together. Fig. 6 shows both the addition of an upright pair to a horizontal one, and the addition of a horizontal pair to an upright one.

Parallel hierarchical assembly was achieved by starting with enough modules in the tank for the assembly of two 3D structures (i.e. eight modules). While excess modules could have been used to accelerate assembly, this would have hindered experimental imaging and the identification of assembly events. This likely contributed to the long times required for assembly. Pairs of modules were then assembled simultaneously on the top and bottom rows of the substrate. However, because of the human-supervised approach, steps that required the operator’s attention (i.e. identifying state transitions) had to be processed serially. Additionally, the three by three substrate array was not large enough to conduct the second stage of assembly simultaneously. Nonetheless, these experiments demonstrated the capability of the SFA system to achieve parallel hierarchical 3D assembly.

## VI. AUTOMATED ASSEMBLY EXPERIMENTS

The goal of the automated assembly experiments was to demonstrate completely automated assembly of a non-planar 3D structure. This was achieved following a hierarchical approach as in the experiments of Section V, except with pressure sensor feedback in the place of feedback from a human operator (see supplementary movie).

The pressure sensors were used to determine when a module had been attracted to a substrate port. However, the outlet pressure was found to drop significantly only when a

module became perfectly aligned with a substrate port. Thus, the system was not able to detect modules when they were first attracted to the substrate. For this reason, the open-loop subroutines for *Attract* and *Align* had to be combined into one routine that could accomplish both (see Table I). This resulted in slower assembly rates since attracted modules would often be inadvertently rejected from the substrate.

On the other hand, the pressure sensors were very accurate at identifying when adjacent modules had latched because only perfectly mated modules completely blocked the flow through both their ports. Identifying latching visually, on the other hand, was difficult and misidentifications led to assembly errors such as those discussed in Section IV.

One of the consequences of using only pressure sensor feedback for assembly is it becomes much more difficult to create assembly programs to achieve a specific target structure. However, this is a common property of many stochastic assembly systems, including the natural systems they are inspired by. For this reason, many researchers have proposed an alternative view of stochastic assembly. Instead of defining an assembly plan as one would for a deterministic assembly system, we must focus on identifying assembly paths similar to chemical reactions, the rates of which can be tuned to achieve bulk quantities of desired target structures. This is the view taken in these automated assembly experiments.

We have tested three assembly programs, recorded all of the resulting assembly/disassembly paths and recorded the rates of each (Fig. 7). These statistics were collected over multiple 30 to 40 minute runs of each program.

In Program 1, the assembly tank is populated with individual modules, which are attracted to two adjacent substrate locations where assembly occurs. All of the other assembly ports act as agitation sources. This program was run for a total of 1h 37m. Over this period, we observed the assembly of two modules into pairs at a rate of 7.39 per hour, while the reverse reaction (disassembly of a pair into individual modules) occurred at a rate of 3.70 per hour. Thus, pairs were assembled at a net rate of 3.69 per hour. Occasionally, a pair would be attracted upright and assembled to a third cube to form a triad. This reaction occurred at a much slower net rate of 0.61 per hour. Thus, the primary result of Program 1 was to assemble individual modules into pairs.

Program 2 was also tested on a tank populated with individual modules, but unlike Program 1, three substrate positions forming an L-shape were identified as outlet ports. This program was tested over the course of 1h 46m. One of the consequences of the *Attract/Align* subroutine for programs with three outlet ports is that often the agitation of assembled module required to allow a third module to align would inadvertently reject the incomplete structure from the substrate. Thus, this program frequently resulted in the assembly of module pairs, and less frequently in L-shapes. Nonetheless, the net assembly rate of L-shapes (1.13 per hour) was almost twice that of Program 1, while the net assembly rate of pairs (2.82 per hour) was approximately one fourth.

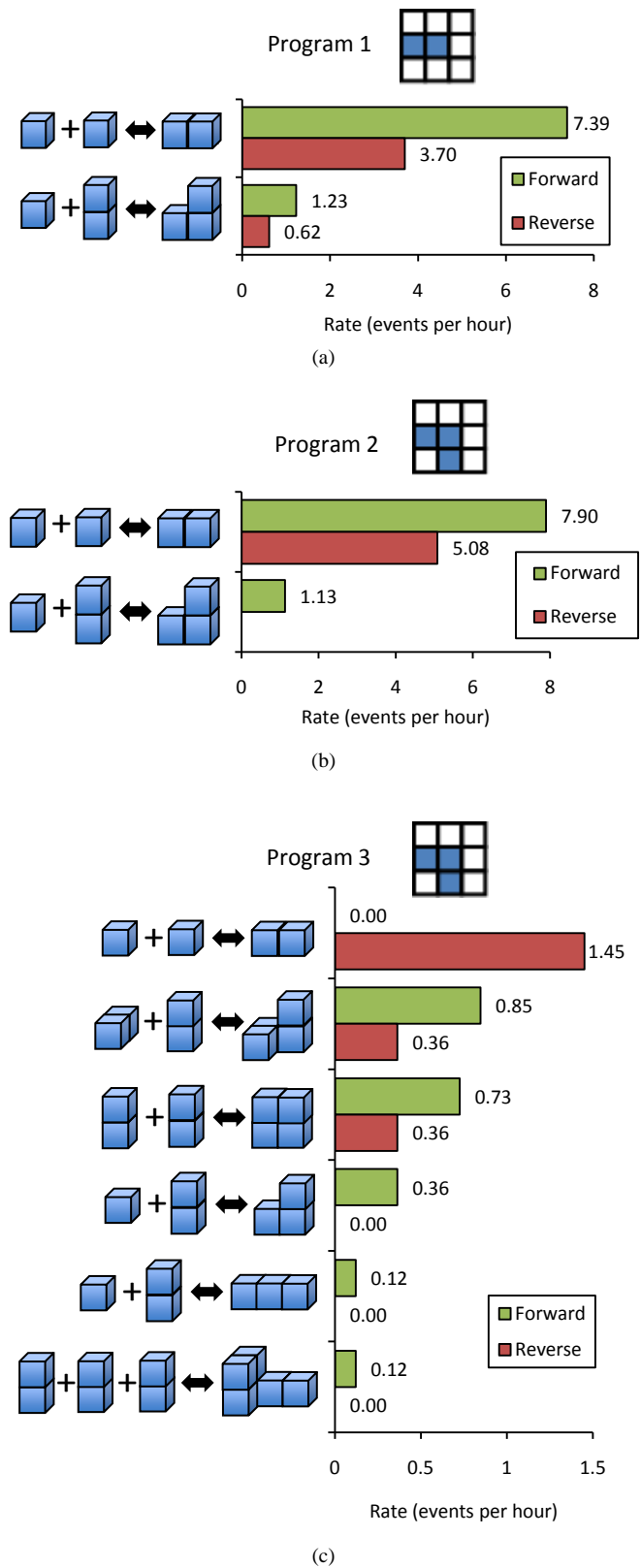


Fig. 7. Assembly rates. Bar graphs indicate the experimentally determined rates of various assembly events ('reactions') for three assembly programs. The light bars indicate the rates of the forward reaction, while the dark bars indicate reverse reaction rates. Dark squares in the schematic to the top-right of each graph indicate the configuration of substrate ports acting as outlets in each case.

Finally, Program 3 involved the same outlet pattern as Program 2, but applied to a tank populated with cube pairs. From Fig. 7(c) we see that this program resulted in a range of possible reactions with a variety of reaction rates. Because of this, the program was run many more times than the others (a total of 8h 16m). Since the tank was repopulated with cube pairs for each run, the most common reaction was the disassembly of these pairs into individual modules. However, the second most popular reaction was the assembly of pairs into the same nonplanar 3D structure assembled in the experiments of Section V.

## VII. DISCUSSION AND CONCLUSIONS

In this paper we have presented a system for SFA and examined its capabilities with three sets of experiments. The first set of experiments demonstrated the ability of the system to achieve repeatable 3D assembly of four-module structures. This was achieved using a human operator to identify assembly events, although in principle this could be done with a vision system.

The second set of experiments demonstrated the parallel hierarchical assembly of two identical 3D structures. This approach offers a potential route to overcoming the slow assembly rates inherent with SFA approaches.

In the third set of experiments, we used pressure sensor feedback to achieve completely automated 3D assembly. Three assembly programs were tested over the course of many hours and the resulting ‘reactions’ and associated reaction rates were recorded. These reactions resulted in different net assembly rates for different structures, suggesting that it may be possible to identify programs to achieve significant proportions of a desired target structure. However, a relatively small number of experiments were conducted, thus more experiments would be necessary to be able to make specific predictions with confidence.

## REFERENCES

- [1] S. C. Goldstein, J. D. Campbell, and T. C. Mowry, “Programmable matter,” *Computer*, vol. 38, iss. 6, pp 99-101, May 2005.
- [2] K. Gilpin, K. Kotay, D. Rus, I. Vasilescu. “Miche: modular shape formation by self-disassembly,” *Int. J. Robotics Research*, vol. 27, pp. 345-372, Mar. 2008.
- [3] E. Hawkes, B. An, N. M. Benbernou, H. Tanaka, S. Kim, E. D. Demaine, D. Rus, and R. J. Wood. “Programmable matter by folding,” *Proc. Natl. Acad. Sci.*, vol. 107, pp 12441-12445, July 2010.
- [4] P. J. White, M. L. Posner and M. Yim, “Strength analysis of miniature folded right angle tetrahedron chain programmable matter,” in *Proc. IEEE Int. Conf. Robotics and Automation*, Anchorage AK, May 2010, pp. 2785-2790.
- [5] P. J. White, K. Kopanski, H. Lipson, “Stochastic self-reconfigurable cellular robotics,” in *Proc. IEEE Int. Conf. Robot. and Autom.*, New Orleans, 2004, vol. 3, pp. 2888-2893.
- [6] E. Klavins, “Programmable self-assembly,” *IEEE Control Systems Magazine*, vol. 27, no. 4, pp. 43-56, Aug. 2007.
- [7] S. Griffith, D. Goldwater, J. M. Jacobson, “Robotics: self-replication from random parts,” *Nature* vol. 437, p. 636, Sept. 2005.
- [8] P. White, V. Zykov, J. Bongard, and H. Lipson, “Three dimensional stochastic reconfiguration of modular robots,” in *Proc. Robotics Science and Systems*, Cambridge, 2005, pp. 161-168.
- [9] V. Zykov, and H. Lipson H., “Experiment design for stochastic three-dimensional reconfiguration of modular robots”, in *Proc. IEEE Int.*

*Conf. Intelligent Robots and Systems, Self-Reconfigurable Robotics Workshop*, San Diego CA, Oct. 2007.

- [10] M. T. Tolley, M. Krishnan, D. Erickson, and H. Lipson, “Dynamically programmable fluidic assembly,” *Appl. Phys. Lett.*, vol. 93, 254105, Dec. 2008.
- [11] M. T. Tolley, A. Baisch, M. Krishnan, D. Erickson, and H. Lipson, “Interfacing methods for fluidically-assembled microcomponents”, in *Proc. IEEE Int. Conf. Microelectromechanical Systems*, Tucson AZ, Jan. 2008, pp. 1073-1076.
- [12] M. T. Tolley, M. Kalontarov, J. Neubert, D. Erickson, and H. Lipson, “Stochastic modular robotic systems: a study of fluidic assembly strategies,” *IEEE T. Robotics*, vol. 26, pp. 1552-3098.
- [13] M. T. Tolley and H. Lipson, “On-line assembly planning for stochastically reconfigurable systems,” *Int. J. Robotics Research*, online first, Mar. 2011.
- [14] M. T. Tolley and H. Lipson, “Fluidic Manipulation for Scalable Stochastic 3D Assembly of Modular Robots,” in *Proc. IEEE Int. Conf. Robotics and Automation*, Anchorage AK, May 2010, pp. 2473 – 2478.